

CARBONGASES—Retrieval and Analysis of Carbon Dioxide and Methane Greenhouse Gases from SCIAMACHY on Envisat

Oliver Schneising

Abstract CARBONGASES aims at making a contribution to fill the significant gaps in our understanding of the global carbon cycle by improving our knowledge about the regional sources and sinks of the two most important anthropogenic greenhouse gases, carbon dioxide and methane. To this end, global multi-year satellite data sets, namely column-averaged dry air mole fractions of carbon dioxide and methane retrieved from the SCIAMACHY instrument onboard the European environmental satellite Envisat are generated. CARBONGASES embodies seven years (2003–2009) of greenhouse gas information derived from European Earth observation data improving and extending pre-existing retrievals to maximise the quantitative information on regional surface fluxes of greenhouse gases which can be inferred from the SCIAMACHY data products using inverse modelling.

Keywords CO₂ • CH₄ • Greenhouse gases sinks and sources • Multi-year data sets

1 Introduction

Carbon dioxide (CO₂) and methane (CH₄) are the two most important anthropogenic greenhouse gases and contribute to global climate change. Both gases have increased significantly since the start of the Industrial Revolution and are now about 40 and 150 %, respectively, higher compared to the pre-industrial levels

O. Schneising (✉)

Institute of Environmental Physics (IUP), University of Bremen, FB1, Otto-Hahn-Allee 1,
P. O. Box 33 04 40 Bremen D-28334, Germany
e-mail: Oliver.Schneising@iup.physik.uni-bremen.de

[25]. While the CO_2 concentrations have risen steadily during the last decades, atmospheric CH_4 levels were rather stable from 1999 to 2006 [3, 9] before a renewed growth was observed from surface flask measurements since 2007 [10, 18]. Despite their importance, there are still many gaps in our understanding of the sources and sinks of these greenhouse gases [26] and their biogeochemical feedbacks and response in a changing climate, hampering reliable climate predictions. However, theoretical studies have shown that satellite measurements have the potential to significantly reduce surface flux uncertainties by deducing strength and spatiotemporal distribution of the sources and sinks via inverse modelling, if the satellite data are accurate and precise enough [11, 15, 17]. The reduction of regional flux uncertainties requires high sensitivity to near-surface greenhouse gas concentration changes because the variability due to regional sources and sinks is largest in the lowest atmospheric layers.

The SCIAMACHY instrument onboard the European environmental satellite Envisat (launched in 2002) [4, 8] was the first and is now with TANSO onboard GOSAT (launched in 2009) [28] one of only two satellite instrument currently in space enabling the retrieval of carbon dioxide and methane with significant sensitivity in the boundary layer by using measurements of reflected solar radiation in the near-infrared/shortwave-infrared (NIR/SWIR) spectral range. Therefore, SCIAMACHY plays a pioneering role in the relatively new area of greenhouse gas observations from space. OCO-2 (to be launched in 2013) [2] will be another satellite designed to observe atmospheric CO_2 in the same spectral region as SCIAMACHY and TANSO. CarbonSat [5], which is one of two candidates Earth Explorer Opportunity Missions (EE-8) (to be launched in 2018) shall also measure CO_2 and CH_4 in this spectral range. The CARBONGASES project ensures that the era of continuous greenhouse gas observations from space with high sensitivity to near-surface concentration changes starts with the European Envisat satellite.

2 Methodology

The column-averaged dry air mole fractions of carbon dioxide and methane (denoted XCO_2 and XCH_4) are derived using O_2 , CO_2 , and CH_4 vertical columns retrieved from SCIAMACHY nadir spectra of reflected solar radiation in the near-infrared/shortwave-infrared (NIR/SWIR) spectral region with an improved version of the Weighting Function Modified DOAS (WFM-DOAS) algorithm [6, 7, 21–24]. The mole fractions are obtained from the vertical column amounts of the greenhouse gases by normalising with the air column, which can be determined by a simultaneously measured gas with less variability, e.g., O_2 .

WFM-DOAS is a least-squares method based on scaling pre-selected atmospheric vertical profiles. The logarithm of the sun-normalised radiance can be assumed locally as a linear function of the vertical columns under the scaling assumption of the vertical profiles of the absorbing gases if the linearisation point

$\bar{\mathbf{V}}$ is close enough to \mathbf{V} , where the components of vector \mathbf{V} , denoted V_j , are the vertical columns of all trace gases which have absorption lines in the selected fitting window. Hence, the modelled radiation is given by

$$\ln I_{\lambda_l}^{\text{mod}}(\mathbf{V}, \mathbf{b}) = \ln I_{\lambda_l}^{\text{mod}}(\bar{\mathbf{V}}) + \sum_{j=1}^J \left. \frac{\partial \ln I_{\lambda_l}^{\text{mod}}}{\partial V_j} \right|_{\bar{V}_j} \cdot (V_j - \bar{V}_j) + P_{\lambda_l}(\mathbf{b}) \quad (1)$$

with the center wavelength λ_l of detector pixel number l and vector of polynomial coefficients \mathbf{b} of polynomial P . A derivative, also called weighting function, with respect to a vertical column refers thereby to the change of the top-of-atmosphere radiance caused by a scaling of a pre-selected absorber concentration vertical profile.

Since the number of spectral points m in the fitting window is greater than the number n of parameters to retrieve, the problem is overconstrained and a linear least-squares approach is suitable for the retrieval of the desired vertical columns. The radiative transfer model is fitted to the logarithm of the observed sun-normalised radiance I^{obs} by minimising the difference between observation and model, i.e., the Euclidean norm of fit residuum vector **RES** (with components RES_l), for all spectral points λ_l simultaneously. The least-squares WFM-DOAS equation is then

$$\sum_{l=1}^m \left(\ln I_{\lambda_l}^{\text{obs}} - \ln I_{\lambda_l}^{\text{mod}}(\hat{\mathbf{V}}, \hat{\mathbf{b}}) \right)^2 \equiv \|\mathbf{RES}\|_2^2 \rightarrow \min. \quad (2)$$

where the model is given by (1) and the fit parameter vectors or vector components are indicated by a hat. The fit parameters are the desired trace gas vertical columns \hat{V}_j and the polynomial coefficients. An additional fit parameter also used (but for simplicity omitted in the equations given above) is the shift (in Kelvin) of a pre-selected temperature profile. This fit parameter has been added in order to take the temperature dependence of the trace gas absorption cross-sections into account.

The least-squares problem can also be expressed in the following vector/matrix notation. Given a forward model by

$$\mathbf{y} = \mathbf{A}\mathbf{x} + \mathbf{e} \quad (3)$$

with m -dimensional measurement vector \mathbf{y} , n -dimensional state vector \mathbf{x} , ($m \times n$) weighting function matrix \mathbf{A} , and model error \mathbf{e} , the most probable inference $p(\mathbf{x}|\mathbf{y})$ is obtained by minimising $\chi^2 = \|\mathbf{y} - \mathbf{A}\mathbf{x}\|_2^2$ with respect to \mathbf{x} . The solution is

$$\hat{\mathbf{x}} = \mathbf{C}_x \mathbf{A}^T \mathbf{y}, \quad \mathbf{C}_x = (\mathbf{A}^T \mathbf{A})^{-1} \quad (4)$$

where \mathbf{C}_x is the covariance matrix of solution $\hat{\mathbf{x}}$.

In order to avoid time-consuming on-line radiative transfer simulations, a fast look-up table scheme has been implemented. The pre-computed spectral radiances and their derivatives (e.g., with respect to trace gas concentration and temperature profile changes) depend on solar zenith angle, surface elevation (pressure), surface albedo, and water vapour amount (to consider possible non-linearities caused by the high variability of atmospheric water vapour). These reference spectra are

computed with the radiative transfer model SCIATRAN [20] for assumed (e.g., climatological) “mean” columns \bar{V} solely depending on surface elevation. Multiple scattering is fully taken into account.

3 Results

All available SCIAMACHY spectra (Level 1b version 6 converted to Level 1c by the ESA SciaL1C tool using the standard calibration) for the years 2003–2009 have been processed using the improved retrieval algorithm WFM-DOAS version 2.0/2.1 [23, 24]. An overview of the long-term global data sets is shown in Figs. 1 and 2. Selected carbon dioxide and methane results are discussed in the following subsections.

3.1 Carbon Dioxide

The carbon dioxide mole fractions as a function of latitude and time are shown in Fig. 1 demonstrating the pronounced seasonal cycle due to growing and decaying vegetation and the steady increase of atmospheric carbon dioxide primarily caused by the burning of fossil fuels.

Growth rate and seasonal cycle. To examine the increase with time and the seasonal cycle more quantitatively, the SCIAMACHY results are compared to the CarbonTracker release 2010 assimilation system [16] based on monthly data. The CarbonTracker XCO₂ fields as used for this study have been sampled in space and time as the SCIAMACHY satellite instrument measures. The SCIAMACHY altitude sensitivity has been taken into account by applying the SCIAMACHY CO₂ column averaging kernels to the CarbonTracker CO₂ vertical profiles. The retrieved continuous increase with time is consistent with CarbonTracker. An analysis of global, hemispheric, and smaller zonal averages demonstrates that the annual mean increase agrees with the assimilation system within the error bars amounting to about 2 ppm/year, respectively.

For the Northern Hemisphere we also find good agreement of the phase of the CO₂ seasonal cycle with the model resulting in a pronounced correlation of the two data sets ($r = 0.98$). In contrast to the Northern Hemisphere, the seasonal cycle is less pronounced in the Southern Hemisphere and systematic phase differences are observed leading to a somewhat smaller correlation ($r = 0.91$) which is, nevertheless, quite high due to the observed consistent increase with time in both data sets. The discrepancy of the phases in the Southern Hemisphere can probably be ascribed to a large extent to the higher weight on ground scenes with occurrences of subvisual thin cirrus (induced by the restriction to land and the smaller land fraction compared to the Northern Hemisphere). Cirrus clouds are not

Fig. 1 Overview of the long-term global WFMDv2.1 carbon dioxide data set; shown are column-averaged dry air mole fractions as a function of latitude and time. In addition to the pronounced seasonal cycle due to growing and decaying vegetation, the steady increase of atmospheric carbon dioxide primarily caused by the burning of fossil fuels can be clearly observed

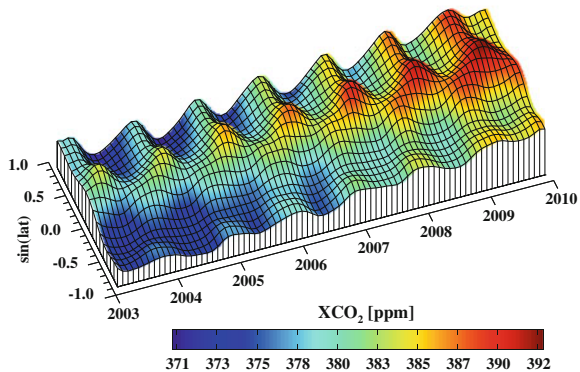
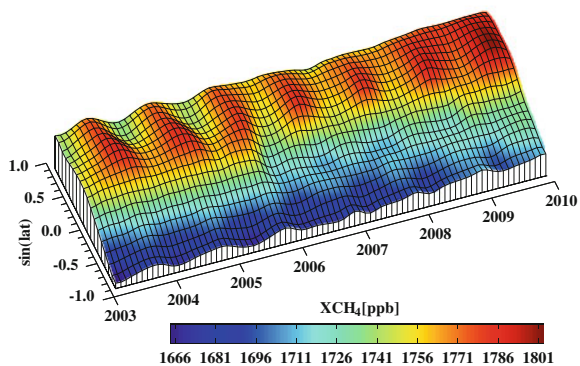


Fig. 2 Overview of the long-term global WFMDv2.0.2 methane data set; shown are column-averaged dry air mole fractions as a function of latitude and time. Clearly visible is the interhemispheric gradient and the renewed methane growth in recent years



explicitly considered in WFM-DOAS yet and are hence a potential error source leading to a possible overestimation of the carbon dioxide mole fractions for scenes with high subvisual cirrus fraction [21]. Although cloud parameters are not included in the state vector of the current WFM-DOAS version, the influence of thin clouds on the retrievals is minimised resulting in much better agreement with CarbonTracker compared to the previous WFM-DOAS version especially in the Southern Hemisphere. The achieved reduction of the amplitude of the seasonal cycle is presumably a consequence of the interaction of the more realistic default aerosol scenario used in the forward model, improved spectroscopy and calibration, and the change-over to the SCIAMACHY Absorbing Aerosol Index to filter strongly aerosol contaminated scenes, in particular desert dust storms.

From the analysis of several zonal averages it can be concluded that the mean amplitude of the retrieved seasonal cycle is typically about 1 ppm larger than for CarbonTracker deriving for example 4.3 ± 0.2 ppm for the Northern Hemisphere and 1.4 ± 0.2 ppm for the Southern Hemisphere from the SCIAMACHY data.

In contrast to the growth rates, the seasonal cycle amplitude differences between SCIAMACHY and CarbonTracker are significant. The less pronounced seasonal cycle of CarbonTracker compared to the satellite data might be explainable to some extent by a too low net ecosystem exchange (NEE) between the atmosphere and the terrestrial biosphere in the underlying Carnegie-Ames Stanford Approach (CASA) biogeochemical model [13]. On the other hand, it cannot be completely excluded that undetected seasonally varying thin cirrus clouds might also contribute to some extent to the observed differences in the seasonal cycle amplitudes.

Boreal carbon uptake. Another related aspect analysed is the boreal forest carbon uptake during the growing season and its local partitioning between North America and Eurasia. To this end, longitudinal gradients of atmospheric carbon dioxide are studied during May–August (the period between the maximum and minimum of the seasonal cycle), which are the basic signals to infer regional fluxes, using a region consisting of equally sized slices in North America and Eurasia covering the bulk of the boreal forest area of the planet. When an air parcel flows over the boreal forest, more and more carbon is steadily taken up by the growing vegetation leading to a gradient parallel to wind direction with smaller values at the endpoint compared to the starting point. Due to the fact that the prevailing wind direction in mid- to high-latitudes is from west to east, one would expect a negative west-to-east longitudinal gradient for the considered region because the air masses are mainly moving according to this wind direction over the uptake region.

The gradients are derived by calculating meridional averages of seasonally averaged (May–August) SCIAMACHY and CarbonTracker XCO₂ as a function of longitude (in 0.5° bins) and linear fitting the corresponding west-to-east gradient weighted according to the standard deviations of the meridional averages. The associated error is derived from the square root of the covariance of the linear fit parameter. This investigation of the boreal forest carbon uptake during the growing season shows good agreement between SCIAMACHY and CarbonTracker concerning the annual variations of the gradients (see Fig. 3). While there is also very good quantitative agreement of the gradients for the overall region, there are systematic differences if both slices are analysed separately suggesting stronger American and weaker Eurasian uptake. However, these differences are not significant because both data sets agree within their error bars.

The suggested difference between CarbonTracker and SCIAMACHY concerning the relative strengths of the Eurasian and North American boreal forest uptake might be linked to the recent finding that modified CASA flux strengths and timings of the seasonal cycle introduce differences in corresponding gradients [12]. Therefore, a potential regional timing error in the onset of the forest uptake in the CASA model might contribute to the observed difference between CarbonTracker and SCIAMACHY. This potential contribution to the differences can be minimised by averaging over shorter time periods starting later. Actually, the restriction to June–August reduces the differences between CarbonTracker and SCIAMACHY concerning the relative regional uptake strengths to some extent, but the qualitative findings concerning regional partitioning remain the same.

Fig. 3 Annual west-to-east longitudinal XCO_2 gradients from SCIAMACHY (black) and CarbonTracker (red) for boreal forests during the growing season. The examined boreal forest region is composed of two equally sized regions in North America and Eurasia. The gradients and associated errors are illustrated for the overall region and the North American and Eurasian slice separately

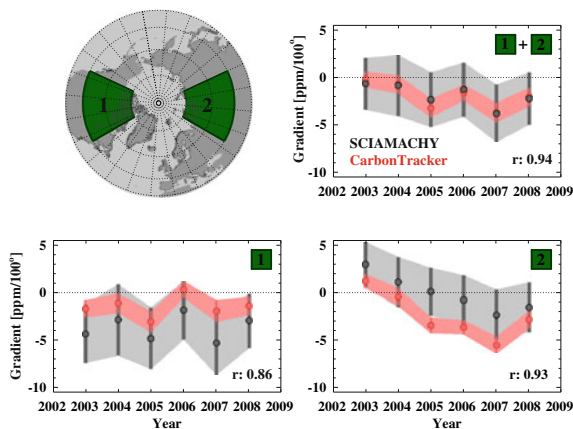
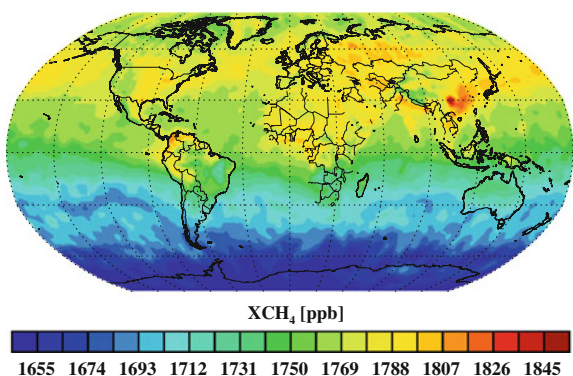


Fig. 4 Seven years mean (2003–2009) of retrieved SCIAMACHY methane. Clearly visible are major methane source regions like the Sichuan Basin in China and the interhemispheric gradient



3.2 Methane

The methane mole fractions as a function of latitude and time are shown in Fig. 2. The retrieved methane results show that after years of stability, atmospheric methane has started to rise again in recent years which is consistent with surface measurements [10, 18]. Major methane source regions like the Sichuan Basin in China which is famous for rice cultivation and the interhemispheric gradient with larger methane concentrations in the Northern Hemisphere are clearly visible in the data (see Fig. 4).

Due to proceeding detector degradation in the spectral range used for the methane column retrieval, the results since November 2005, when the impact of solar protons resulted in random telegraph noise of the detector pixel measuring

the strongest CH_4 absorption in the Q-branch of the $2\nu_3$ band, are of reduced quality manifesting itself in particular by larger scatter. There are also indications for possible systematic effects; e.g., Fig. 2 suggests a potential negative tropical bias since that time.

Renewed growth. To examine the renewed methane growth in recent years more quantitatively the SCIAMACHY results are compared to the TM5-4DVAR inverse model [1, 14], which is optimised by assimilating highly accurate surface measurements at background sites from the NOAA/ESRL network, taking the SCIAMACHY averaging kernels into account. The global comparison with SCIAMACHY based on monthly data shows a pronounced correlation ($r = 0.84$) and a consistent anomaly of about 7 ppb/year since 2007.

Analysing the results for several zonal averages, the largest increase of the SCIAMACHY data is observed for the tropics and northern mid- and high-latitudes. This is consistent with [10] and the speculation that possible drivers of this renewed increase are positive anomalies of arctic temperatures and tropical precipitation.

Due care has been exercised to minimise the influence of detector degradation on the quantitative estimate of this anomaly. In this context it has to be pointed out that a static pixel mask is used since November 2005 including the entire time period of renewed increase to ensure that the observed growth is not artificially introduced by proceeding detector degradation.

3.3 Validation

From the validations with ground-based Fourier Transform Spectroscopy (FTS) measurements and comparisons with model results (CarbonTracker XCO_2 and TM5-4DVAR XCH_4) at eight Total Carbon Column Observing Network (TCCON) sites [27] distributed over Europe, America, and Australia, realistic error estimates of the satellite data are provided [24] and summarised in Table 1. Such validation is a prerequisite to assess the suitability of data sets for their use in inverse modelling. The different averaging kernels of SCIAMACHY and FTS influencing the respective absolute amounts of retrieved seasonal variability and annual increase have to be taken into account appropriately. According to [19] this

Table 1 Error characterisation of the WFM-DOAS v2.1 XCO_2 and v2.0.2 XCH_4 data products

	XCO_2 (ppm)		XCH_4 (ppb)	
	SCIA-FTS	SCIA-CT	SCIA-FTS	SCIA-TM5
Global offset	0.8	0.1	−0.3	15
Regional precision	2.2	2.2	18 (13; 16)	16 (12; 13)
Relative accuracy	1.1	1.2	19 (1.3; 21)	7.7 (2.8; 15)

The values in brackets for methane correspond to the two periods before and after the pixel mask change due to detector degradation at the beginning of November 2005 revealing the worsening of retrieval quality afterwards

can be achieved by adjusting the measurements for a common a priori profile. For simplicity, the modelled profiles (CarbonTracker for XCO₂ and TM5-4DVAR for XCH₄) are used as common a priori enabling direct comparability of SCIAMACHY, FTS, and the corresponding model results:

$$c_{adj} = \hat{c} + \frac{1}{p_0} \sum_l (1 - A^l) (x_{mod}^l - x_a^l) \Delta p^l \quad (5)$$

In this equation, \hat{c} represents the column-averaged mole fraction retrieved by SCIAMACHY or FTS, l is the index of the vertical layer, A^l the column averaging kernel, x_a^l the a priori mole fraction, and x_{mod}^l the modelled mole fraction (and new common a priori) of layer l . p^l is the pressure difference between the upper and lower boundary of layer l and p_0 denotes surface pressure.

The relevant parameters for quality assessment are the global offset which is defined as the averaged mean difference to the reference data set over all sites, the regional precision relative to the reference which is the averaged standard deviation of the differences, and the relative accuracy which is the standard deviation of the mean differences to FTS or model simulations. The results are summarised in Table 1 indicating that SCIAMACHY carbon dioxide retrievals potentially provide valuable information for regional source/sink determination by inverse modelling techniques in places where surface flask observations are sparse and suggesting that the SCIAMACHY methane data are suitable for global inverse modelling at least before November 2005.

References

1. Bergamaschi P, Frankenberg C, Meirink JF, Krol M, Villani MG, Houweling S, Dentener F, Dlugokencky EJ, Miller JB, Gatti LV, Engel A, Levin I (2009) Inverse modeling of global and regional CH₄ emissions using SCIAMACHY satellite retrievals. *J Geophys Res* 114:D22301. doi: [10.1029/2009JD012287](https://doi.org/10.1029/2009JD012287)
2. Boesch H, Baker D, Connor B, Crisp D, Miller C (2011) Global characterization of CO₂ column retrievals from shortwave-infrared satellite observations of the orbiting carbon observatory-2 mission. *Remote Sens* 2011:270–304. doi: [10.3390/rs3020270](https://doi.org/10.3390/rs3020270)
3. Bousquet P, Ciais P, Miller JB, Dlugokencky EJ, Hauglustaine DA, Prigent C, Van der Werf GR, Peylin P, Brunke E-G, Carouge C, Langenfelds RL, Lathiere J, Papa F, Ramonet M, Schmidt M, Steele LP, Tyler SC, White J (2006) Contribution of anthropogenic and natural sources to atmospheric methane variability. *Nature* 443:439–443. doi:[10.1038/nature05132](https://doi.org/10.1038/nature05132)
4. Bovensmann H, Burrows JP, Buchwitz M, Frerick J, Noël S, Rozanov VV, Chance KV, Goede A (1999) SCIAMACHY—Mission objectives and measurement modes. *J Atmos Sci* 56:127–150
5. Bovensmann H, Buchwitz M, Burrows JP, Reuter M, Krings T, Gerilowski K, Schneising O, Heymann J, Tretnar A, Erzinger J (2010) A remote sensing technique for global monitoring of power plant CO₂ emissions from space and related applications. *Atmos Meas Tech* 3:781–811. doi: [10.5194/amt-3-781-2010](https://doi.org/10.5194/amt-3-781-2010)
6. Buchwitz M, de Beek R, Burrows JP, Bovensmann H, Warneke T, Notholt J, Meirink JF, Goede APH, Bergamaschi P, Körner S, Heimann M, Schulz A (2005) Atmospheric methane

- and carbon dioxide from SCIAMACHY satellite data: initial comparison with chemistry and transport models. *Atmos Chem Phys* 5:941–962. doi:[10.5194/acp-5-941-2005](https://doi.org/10.5194/acp-5-941-2005)
7. Buchwitz M, de Beek R, Noël S, Burrows JP, Bovensmann H, Bremer H, Bergamaschi P, Körner S, Heimann M (2005) Carbon monoxide, methane and carbon dioxide columns retrieved from SCIAMACHY by WFM-DOAS: year 2003 initial data set. *Atmos Chem Phys* 5:3313–3329. doi:[10.5194/acp-5-3313-2005](https://doi.org/10.5194/acp-5-3313-2005)
 8. Burrows JP, Hölzle E, Goede APH, Visser H, Fricke W (1995) SCIAMACHY—Scanning imaging absorption spectrometer for atmospheric chartography. *Acta Astronautica* 35:445–451
 9. Dlugokencky EJ, Houweling S, Masarie KA, Lang PM, Miller JB, Tans PP (2003) Atmospheric methane levels off: temporary pause or a new steady-state? *Geophys Res Lett* 30. doi:[10.1029/2003GL018126](https://doi.org/10.1029/2003GL018126)
 10. Dlugokencky EJ, Bruhwiler L, White JWC, Emmons LK, Novelli PC, Montzka SA, Masarie KA, Lang PM, Crotwell AM, Miller JB, Gatti LV (2009) Observational constraints on recent increases in the atmospheric CH₄ burden. *Geophys Res Lett* 36:L18803. doi: [10.1029/2009GL039780](https://doi.org/10.1029/2009GL039780)
 11. Houweling S, Breon F-M, Aben I, Rödenbeck C, Gloor M, Heimann M, Ciais P (2004) Inverse modeling of CO₂ sources and sinks using satellite data: a synthetic inter-comparison of measurement techniques and their performance as a function of space and time. *Atmos Chem Phys* 4:523–538. doi: [10.5194/acp-4-523-2004](https://doi.org/10.5194/acp-4-523-2004)
 12. Keppel-Aleks G, Wennberg PO, Schneider T (2011) Sources of variations in total column carbon dioxide. *Atmos Chem Phys* 11:3581–3593. doi:[10.5194/acp-11-3581-2011](https://doi.org/10.5194/acp-11-3581-2011)
 13. Keppel-Aleks G, Wennberg PO, Washenfelder RA, Wunch D, Schneider T, Toon GC, Andres RJ, Blavier J-F, Connor B, Davis KJ, Desai AR, Messerschmidt J, Notholt J, Roehl CM, Sherlock V, Stephens BB, Vay SA, Wofsy SC (2011) The imprint of surface fluxes and transport on variations in total column carbon dioxide. *Biogeosci. Discuss* 8:7475–7524. doi:[10.5194/bgd-8-7475-2011](https://doi.org/10.5194/bgd-8-7475-2011)
 14. Meirink JF, Bergamaschi P, Krol MC (2008) Four-dimensional variational data assimilation for inverse modelling of atmospheric methane emissions: method and comparison with synthesis inversion. *Atmos Chem Phys* 8:6341–6353. doi:[10.5194/acp-8-6341-2008](https://doi.org/10.5194/acp-8-6341-2008)
 15. Miller CE, Crisp D, DeCola PL, Olsen SC, Randerson JT, Michalak AM, Alkhaled A, Rayner P, Jacob DJ, Suntharalingam P, Jones DBA, Denning AS, Nicholls ME, Doney SC, Pawson S, Boesch H, Connor BJ, Fung IY, O'Brien D, Salawitch RJ, Sander SP, Sen B, Tans P, Toon GC, Wennberg PO, Wofsy SC, Yung YL, Law RM (2007) Precision requirements for space-based X_{CO₂} data. *J Geophys Res* 112:D10314. doi: [10.1029/2006JD007659](https://doi.org/10.1029/2006JD007659)
 16. Peters W, Jacobson AR, Sweeney C, Andrews AE, Conway TJ, Masarie K, Miller JB, Bruhwiler LMP, Pétron G, Hirsch AI, Worthy DEJ, van der Werf GR, Randerson JT, Wennberg PO, Krol MC, Tans PP (2007) An atmospheric perspective on North American carbon dioxide exchange: CarbonTracker, Proceedings of the National Academy of Sciences (PNAS) of the United States of America 104:18925–18930
 17. Rayner PJ, O'Brien DM (2001) The utility of remotely sensed CO₂ concentration data in surface inversions. *Geophys Res Lett* 28:175–178
 18. Rigby M, Prinn RG, Fraser PJ, Simmonds PG, Langenfelds RL, Huang J, Cunnold DM, Steele LP, Krummel PB, Weiss RF, O'Doherty S, Salameh PK, Wang HJ, Harth CM, Mühle J, Porter LW (2008) Renewed growth of atmospheric methane. *Geophys Res Lett* 35:L22805. doi:[10.1029/2008GL036037](https://doi.org/10.1029/2008GL036037)
 19. Rodgers CD (2000) Inverse methods for atmospheric sounding: theory and practice. World Scientific Publishing, Singapore
 20. Rozanov VV, Buchwitz M, Eichmann K-U, de Beek R, Burrows JP (2002) SCIATRAN—a new radiative transfer model for geophysical applications in the 240–2400 nm spectral region: The pseudo-spherical version. *Adv Space Res* 29:1831–1835
 21. Schneising O, Buchwitz M, Burrows JP, Bovensmann H, Reuter M, Notholt J, Macatangay R, Warneke T (2008) Three years of greenhouse gas column-averaged dry air mole fractions retrieved from satellite—Part 1: Carbon dioxide. *Atmos Chem Phys* 8:3827–3853. doi:[10.5194/acp-8-3827-2008](https://doi.org/10.5194/acp-8-3827-2008)

22. Schneising O, Buchwitz M, Burrows JP, Bovensmann H, Bergamaschi P, Peters W (2009) Three years of greenhouse gas column-averaged dry air mole fractions retrieved from satellite—Part 2: Methane. *Atmos Chem Phys* 9:443–465. doi:[10.5194/acp-9-443-2009](https://doi.org/10.5194/acp-9-443-2009)
23. Schneising O, Buchwitz M, Reuter M, Heymann J, Bovensmann H, Burrows JP (2011) Long-term analysis of carbon dioxide and methane column-averaged mole fractions retrieved from SCIAMACHY. *Atmos Chem Phys* 11:2863–2880. doi:[10.5194/acp-11-2863-2011](https://doi.org/10.5194/acp-11-2863-2011)
24. Schneising O, Bergamaschi P, Bovensmann H, Buchwitz M, Burrows JP, Deutscher NM, Griffith DWT, Heymann J, Macatangay R, Messerschmidt J, Notholt J, Rettinger M, Reuter M, Sussmann R, Toon GC, Velazco VA, Warneke T, Wennberg PO, Wunch D (2011) Atmospheric greenhouse gases retrieved from SCIAMACHY: Comparison to ground-based FTS measurements and model results. *Atmos Chem Phys Discuss* 11:28713–28745. doi:[10.5194/acpd-11-28713-2011](https://doi.org/10.5194/acpd-11-28713-2011)
25. Solomon S, Qin D, Manning M, Chen Z, Marquis M, Averyt KB, Tignor M, and Miller HL (eds) (2007) Climate change 2007: the physical science basis, contribution of working group I to the fourth assessment report of the intergovernmental panel on climate change (IPCC). Cambridge University Press
26. Stephens BB, Gurney KR, Tans PP, Sweeney C, Peters W, Bruhwiler L, Ciais P, Ramonet M, Bousquet P, Nakazawa T, Aoki S, Machida T, Inoue G, Vinnichenko N, Lloyd J, Jordan A, Heimann M, Shibistova O, Langenfelds RL, Steele LP, Francey RJ, Denning AS (2007) Weak northern and strong tropical land carbon uptake from vertical profiles of atmospheric CO₂. *Science* 316:1732–1735. doi: [10.1126/science.1137004](https://doi.org/10.1126/science.1137004)
27. Wunch D, Toon GC, Blavier J-FL, Washenfelder RA, Notholt J, Connor BJ, Griffith DWT, Sherlock V, Wennberg PO (2011) The total carbon column observing network. *Phil Trans R Soc A* 369:2087–2112. doi:[10.1098/rsta.2010.0240](https://doi.org/10.1098/rsta.2010.0240)
28. Yokota T, Yoshida Y, Eguchi N, Ota Y, Tanaka T, Watanabe H, Maksyutov S (2009) Global concentrations of CO₂ and CH₄ retrieved from GOSAT: first preliminary results. *SOLA* 5:160–163. doi: [10.2151/sola.2009-041](https://doi.org/10.2151/sola.2009-041)

Remote Sensing Advances for Earth System Science
The ESA Changing Earth Science Network: Projects
2009-2011

Fernández-Prieto, D.; Sabia, R.

2013, VII, 103 p. 44 illus., 39 illus. in color., Softcover

ISBN: 978-3-642-32520-5